Channel Energy Based Estimation of Target Trajectories Using Distributed Sensors with Low Communication Rate

Christian R. Berger, *Member, IEEE,* Sora Choi, *Student Member, IEEE,* Shengli Zhou, *Member, IEEE,* and Peter Willett, *Fellow, IEEE*

***Abstract*—Sensor localization using channel energy measurements of distributed sensors has been studied in various scenarios. However, it is usually assumed that the target does not move significantly during the time needed to collect and process the data from the sensors. We want to estimate the trajectory of a moving target using a network of distributed sensors that measure only the received signal strength (RSS), sampled and as a function of time, without knowledge of the target amplitude/source level. To reduce the communication load, sensors communicate a reduced data set to the fusion center (FC), generated through local processing. It consists of three characteristic parameters: i) the maximum measured amplitude, corresponding to the closest-point-of-approach (CPA); ii) the corresponding time index; and iii) the time it takes for the amplitude to diminish by 6 dB relative to the CPA. To generate the reduced data sets, each sensor calculates a local maximum likelihood (ML) estimate of its parameters. The accuracy of these local estimates can be reasonably described by their respective Fisher information matrices (FIMs). The FC combines the data transmitted by the sensors using a ML-like formulation based on the local FIMs. This results in a heavily non-linear least-squares problem, which we initialize via geometrical considerations. This approach has a very low communication load, performs comparably to a centralized estimator, and due to the modularized setup, any measurement model at the sensors can be considered.**

***Index Terms*—Source localization, sensor networks, received signal strength (RSS), target tracking.**

I. Introduction

Source localization using sensor arrays has been one of the central problems in radar, sonar, navigation, geophysics, and acoustic tracking. Existing methods are based on three types of physical measurements: time of arrival (TOA), direction of arrival (DOA) or received signal strength (RSS). The first two are used extensively in radar and sonar applications [1], [2], where DOA requires a narrowband signal and, more importantly, a spatial receiver array, while TOA requires either an active setup or highly precise time synchronization between the sensors.

Both these requirements are often not met in sensor networks [3], as sensors are usually small and simple. Various research has therefore suggested alternative approaches to extract target position information from the observed signal: In [4], [5] it is suggested to use signal Doppler information to infer some reduced DOA. In [6], [7] sets of sensors are used to form distributed arrays, while information from more distant sensors can contribute using time difference of arrival (TDOA) information. Note that the use of Doppler information depends strongly on the signal characteristics, coherent processing of distributed measurements needs time synchronization on the order of the signal center frequency, while for TDOA measurements the synchronization needs to be on the order of the signal propagation time.

Therefore, in passive setups, where distributed information cannot be processed coherently, it has been suggested to track targets based on the more easily attained RSS information. This problem has been addressed in [3], [8]–[15] for source localization, where commonly it is assumed that i) the target does not move significantly while the data is collected from the sensors; and ii) a time series of measurements can be averaged to obtain an RSS measurement more robust with respect to temporal variation. The optimal estimator based on all sensor measurements is given by the Maximum Likelihood (ML) formulation; since this leads to a challenging non-linear optimization problem, several works have suggested approaches of solving this challenge: in [9] the authors consider multiple sources and solve the ML formulation using both an expectation-maximization (EM) type algorithm and another iterative approach, in [10] the method of projection-onto-convex-sets (POCS) is applied to solve the optimization problem in a distributed way. To reduce the communication load, in [11]–[13] the authors consider the effect of measurement quantization on localization accuracy in varying setups; [11], [13] also derive the Cramer-Rao lower bound (CRLB) based on quantized measurements.

We are also interested in such a scenario, where distributed sensors have access only to energy readings, but do not have

Manuscript submitted January 7, 2009, revised August 24, 2009, accepted September 18, 2009. This work is supported by the Office of Naval Research, grant N00014-07-1-0429. Part of this work was presented at the 11th International Conference on Information Fusion (FUSION), Cologne, Germany, July 2008. The associate editor coordinating the review of this manuscript and approving it for publication was Dr. Brian Sadler.

C. Berger was with the Department of Electrical and Computer Engineering, University of Connecticut. He is now with the Department of Electrical and Computer Engineering, Carnegie Mellon University, Pittsburgh, PA 15213 USA (e-mail: crberger@andrews.cmu.edu)

S. Choi, S. Zhou, and P. Willett are with the Department of Electrical and Computer Engineering, University of Connecticut, 371 Fairfield Way, U-2157, Storrs, Connecticut 06269 USA (e-mail: {soc07002, shengli, willett}@engr.uconn.edu)

Digital Object Indentifier 00.0000/TSP.2009.000000

the capability to acquire any worthwhile angular information. Instead of considering a relatively slow moving or stationary target as in [3], [8]–[13], we are interested in a more dynamic scenario, where the target moves considerably between measurements. In [15], tracking of a moving target was considered, but the centralized algorithm needs sensors to report frequently, each report leading to one position estimate that can be fed into a tracking algorithm. In this sense, our scenario is most similar to [14], where the communication rate of sensors only allows to transmit limited data, maybe a few data values for the whole time the target is passing through the observable range. In [14] the only parameter extracted from each sensor was the maximum measured amplitude, correponding to the closest-point-of-approach (CPA). We want to extract more information from the RSS meassurement series, but still only a few characteristic values, independent of the length of the raw measurement data vector. Therefore we include a specific measurement model and process measurements at each sensor, while this was assumed to be done already in [14].

The scenario consists of a target moving through a field of distributed sensors, emitting a signal of constant average power, e.g., a jamming signal or engine noise. The target is assumed to move with constant velocity during this time interval and we also assume that the signal propagation time is negligible compared to the target velocity. We consider simple sensors that measure the received energy, recording this information locally over time. Without loss of generality, a free-space attenuation model is adopted, where the RSS is inversely proportional to the distance[1]. The sensors process this data to reduce the communication load; after the target has passed by, the sensors transfer a reduced data set to a fusion center (FC), which estimates the target trajectory. The reduced data set consists of three parameters, which in a noiseless scenario (and assuming constant target motion and free-space attenuation) would completely describe the sensor observations. The three characteristic parameters are:

- the maximum measured amplitude, corresponding to the closest-point-of-approach (CPA);
- the corresponding time index; and
- the time it takes for the amplitude to diminish by 6 dB relative to the CPA.

To generate the reduced data, each sensor calculates the ML estimates of its three parameters based on the received raw data. The accuracy of these local estimates can be reasonably described by the CRLB, which can be easily calculated based on a specific measurement model at the sensors. The FC combines the data transmitted by the sensors using a ML-like formulation, where we simply treat the processed data as Gaussian noise corrupted, with covariance given by the respective CRLBs. This results in a non-linear least-squares problem, which we initialize with several simple estimates generated via geometrical considerations and then apply a generic gradient based optimization scheme to each such starting point. The initial estimates are generated based on the fact that in the noiseless case, two sensors are enough to find four ambiguous solutions, leading to closed form solutions, c.f., [16].

We compare our approach to a centralized ML-estimator and the CRLB based on all raw sensor data. We find the the following:

1) The approach has a very low communication load, as each sensor has to transmit only three parameters, independent of how many local RSS measurements were taken.
2) In comparison to a centralized ML-estimator, having available *all* the raw sensor data, the loss in estimation accuracy is small.
3) Due to the modularized setup, any measurement model at the sensors can be considered, the only necessary change being the implementation of a local ML estimator at the sensors.

Generally the approach can work with a minimum of three sensors to avoid ambiguous solutions, but in case of strongly corrupted or distorted observations at the sensors, more sensors are needed to achieve a solution close to the centralized CRLB.

The rest of this paper is organized as follows: In Section II we describe the problem setup. In Section III we present our approach. Numerical simulation is used to illustrate our approach in Section IV. Then we extend our approach to a fading signal model in Section V, and we conclude in Section VI.

II. Problem Formulation & Centralized Solution

A. Problem Formulation

A target emits or reflects a signal, while moving through a network of N sensors. The sensors are simple and can measure only RSS, but no angular information. We assume a constant velocity model, hence the trajectory of the target $\mathbf{x}(t)$ at time t can be expressed as

$$\mathbf{x}(t) = \mathbf{x}_0 + t\mathbf{v}. \tag{1}$$

Assume that the sensors are located at $\mathbf{x}_s^{(k)}$ for $k = 1, \cdots, N$. Under a free-space signal attenuation model[2] the average received amplitude is expressed by the following equation:

$$a^{(k)}(t_i) \equiv: a_i^{(k)} = \frac{\sqrt{G^{(k)}P_0}}{d_i^{(k)}/d_0} = \frac{\sqrt{P}}{\parallel \mathbf{x}(t_i) - \mathbf{x}_s^{(k)} \parallel}, \tag{2}$$

where $d_i^{(k)} = \parallel \mathbf{x}(t_i) - \mathbf{x}_s^{(k)} \parallel$ is the distance to the k-th sensor, $G^{(k)}$ is the gain of the k-th sensor and P_0 is the emitted energy measured at a reference distance d_0. To simplify, we assume all $G^{(k)} = G$ are equal and define $P = GP_0d_0^2$. Note that this model neglects the signal propagation time, therefore coherent processing across sensors and the use of classical TDOA information is not possible.

[1]This could be extended to include an arbitrary path loss coefficient or even an unkonwn one that would have to additionally estimated.

[2]The free space model can be arbitrary with any path-loss factor $a_i^{(k)} \propto \left(d_i^{(k)}\right)^{-\alpha}$. The form of the ML scheme will change, but the notion does not.

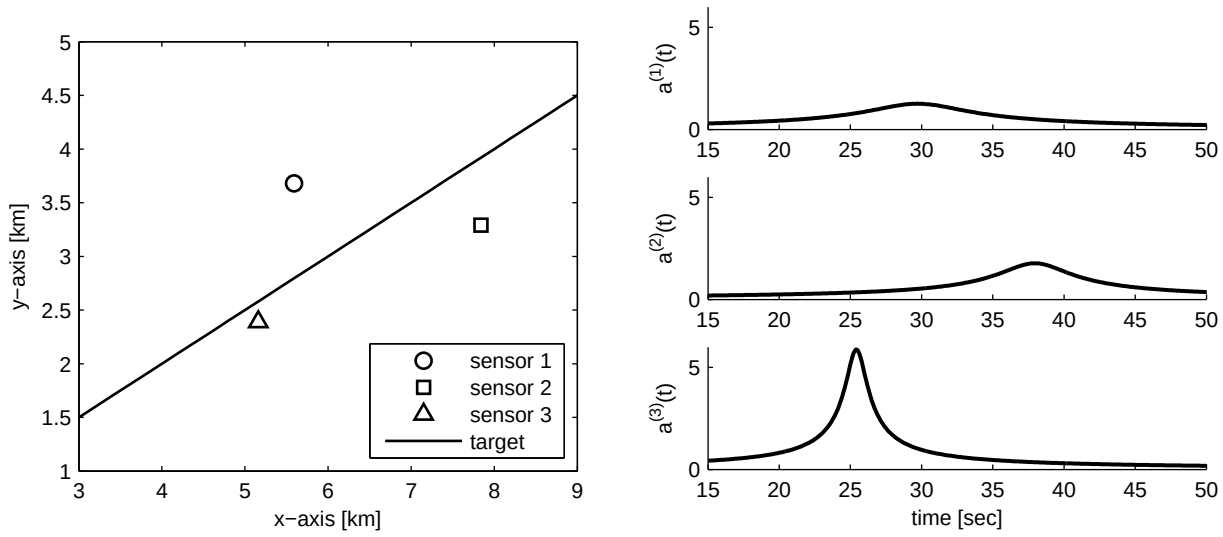

(a) Sensor/Target Locations (b) Sensor Readings

Fig. 1. Example of a target moving through a sensor field: (a) sensor locations relative to target trajectory (target moves from left to right); and (b) noise-free plot of sensor amplitude measurements; each sensor by itself cannot extract any range information without the unkonwn source level, but together we notice that the target passed the closest to sensor three.

B. Conventional Centralized Solution

If there is no information about the amplitude/source level of the target, the vector of unknown target state $\boldsymbol{\theta} = [P, \mathbf{x}_0^T, \mathbf{v}^T]^T$ has to contain P as an additional nuisance paramter[3]. The best centralized estimator is given by the Maximum Likelihood (ML) approach,

$$\boldsymbol{\theta}_{\mathrm{ML}} = \arg\max_{\boldsymbol{\theta}} \prod_{k,i} f\left(r_i^{(k)} \mid \boldsymbol{\theta}\right). \tag{3}$$

In this paper, we will consider explicitly two measurement models – although the approach could be applied to many – the additive white Gaussian noise (AWGN) model and a Rayleigh fading model (Swerling II target). The conditional probability density function $f\left(r_i^{(k)} \mid \boldsymbol{\theta}\right)$ will vary with the model. We will first focus on the AWGN model and consider the more challenging Rayleigh fading model later.

The amplitude measurements under the AWGN model are described by $r_i^{(k)} = a_i^{(k)} + w_i^{(k)}$, where $w_i^{(k)}$ are independent, identical, zero-mean Gaussian noise of variance σ^2. The conditional probability density is accordingly:

$$f\left(r_i^{(k)} \mid \boldsymbol{\theta}\right) = \frac{1}{\sqrt{2\pi}\sigma} \exp\left(-\frac{|r_i^{(k)} - a_i^{(k)}|^2}{2\sigma^2}\right), \tag{4}$$

which can be inserted into the ML estimator in (3) with the amplitude, $a_i^{(k)}$ defined in (2).

Given the above definitions, the Cramer-Rao lower bound (CRLB) on the estimation accuracy of any estimator having available all the raw measurements $\{r_i^{(k)}\}_{k,i}$ can be calculated in a straightforward fashion [17]; the Fisher Information Matrix (FIM) is

$$\begin{aligned} J_{\boldsymbol{\theta}} &= -E\left[\nabla_{\boldsymbol{\theta}} \nabla_{\boldsymbol{\theta}} \log\left\{\prod_{k,i} f\left(r_i^{(k)} \mid \boldsymbol{\theta}\right)\right\}\right] \\ &= \frac{1}{\sigma^2} \sum_{k,i} \left[\nabla_{\boldsymbol{\theta}} a_i^{(k)}\right] \left[\nabla_{\boldsymbol{\theta}} a_i^{(k)}\right]^T, \end{aligned} \tag{5}$$

where we use the gradient of (2) with respect to $\boldsymbol{\theta}$,

$$\nabla_{\boldsymbol{\theta}} a_i^{(k)} = \begin{bmatrix} \frac{\partial a_i^{(k)}}{\partial P} \\ \frac{\partial a_i^{(k)}}{\partial \mathbf{x}_0} \\ \frac{\partial a_i^{(k)}}{\partial \mathbf{v}} \end{bmatrix} = \begin{bmatrix} \frac{1}{2\sqrt{P} d_i^{(k)}} \\ -\frac{\sqrt{P}}{\left[d_i^{(k)}\right]^3}(\mathbf{x}_0 - \mathbf{x}_s^{(k)} + t_i \mathbf{v}) \\ -\frac{t_i \sqrt{P}}{\left[d_i^{(k)}\right]^3}(\mathbf{x}_0 - \mathbf{x}_s^{(k)} + t_i \mathbf{v}) \end{bmatrix}. \tag{6}$$

III. Estimation with Reduced Communication Load

Since in sensor networks we are motivated to reduce the communication overhead and the related expense of energy and bandwidth, we would like to locate and track the target using only a reduced data set of each sensor. In [14], e.g., the authors suggested only utilizing the maximum amplitude measurement of each sensor,

$$a_{\max}^{(k)} :\equiv \max_t a^{(k)}(t), \tag{7}$$

as it is inversely proportional to the distance at the closest-point-of-approach (CPA), $d_{\min}^{(k)}$, i.e,

$$a_{\max}^{(k)} \propto 1/d_{\min}^{(k)} \tag{8}$$

due to the free-space attenuation model.

Using two sensors, the ratio of their maximum amplitudes is the inverse of the ratio of the minimum distances to the target, since they share a common, but unknown, source level. The target trajectory is tangential to two circles centered around the

[3]In the same way it is possible to include an unknown path-loss factor α as another nuisance parameter

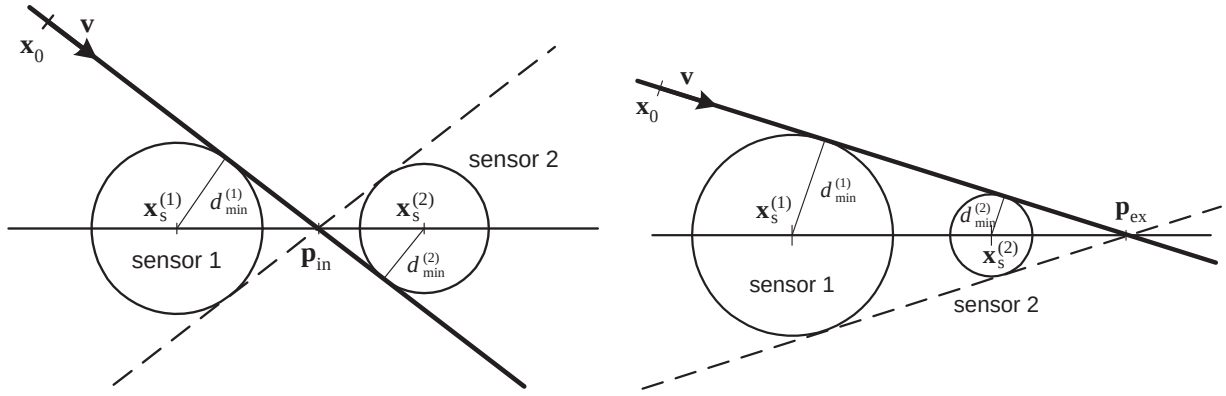

(a) interior solutions (b) exterior solutions

Fig. 2. Given the ratio between the points of closest approach of two sensors, the target trajectory has to pass through one of two possible points ($\mathbf{p}_{\text{in}}$, $\mathbf{p}_{\text{ex}}$); dashed lines are ambiguous solutions (four possible in total).

sensors respectively, their radii given by the minimum distance at the CPA, of which we know only the ratio, not their actual values. As demonstrated in [14], based on a classical geometry theorem by D'Alembert (see e.g. [18]), for a given ratio, this defines two possible points, one of which is part of the target trajectory (see Fig. 2). Using different combinations of two sensors, some information about the target trajectory can be obtained.

The maximum amplitude is related to the minimum distance. However, we believe that more information can be extracted from each sensor. Evaluating the FIM defined in (5) – but for a single sensor only $k = k_0$ – it is singular. This confirms that the information from one sensor only is not enough to estimate the target state. Two vectors $\boldsymbol{\theta}$ and $\boldsymbol{\theta}'$ can produce the same measurements at one sensor, e.g., $\boldsymbol{\theta}' = [\alpha^2 P,\, \mathbf{x}_0^T + \Delta_\alpha \mathbf{x}^T,\, \alpha \mathbf{v}^T]^T$, with $\Delta_\alpha \mathbf{x} = (\alpha - 1)(\mathbf{x}_0 - \mathbf{x}_s^{(k_0)})$, leading to:

$$a_i^{(k_0)} = \frac{\sqrt{P}}{\parallel (\mathbf{x}_0 - \mathbf{x}_s^{(k_0)}) + t_i \mathbf{v} \parallel} \tag{9}$$

$$= \frac{\sqrt{\alpha^2 P}}{\parallel \alpha(\mathbf{x}_0 - \mathbf{x}_s^{(k_0)}) + t_i \alpha \mathbf{v} \parallel}. \tag{10}$$

In words, *a "louder", faster target, farther away leads to the same measurements as the closer, slower target of lower source level*. The information from a single sensor has also angular uncertainty. These two degrees of uncertainty or ambiguity can also be observed in the FIM: given a single sensor only, the FIM has a rank of three, leaving two dimensions undefined in some equivalent 5-dimensional parameter space[4].

Combining the information of two sensors, the FIM has usually full rank (one exeption is if both sensors lie on a line parallel to the target trajectory). As stated before, from the ratio of the maximum amplitudes we can find two points through one of which the target has passed. Additionally we can exploit the time corresponding to the CPA and a measure of how fast the RSS decreases. These parameters imply the velocity of the target. As there are two possible points leading to the same ratio of maximum amplitudes and an ambiguity about the axis connecting the two sensors (c.f. Fig. 2), this will still leave four ambiguous solutions (the FIM is non-singular as there are only finitely many solutions).

[4]Note that we always implicitly assume here that the target has already "passed" the sensor; if the measurements are reported before the CPA, the rank of the FIM will not change, but practically the quality of the measurements will be low – as reflected by a small magnitude of the values of the FIM.

A. Local Sensor Processing

This motivates us to represent the information gathered at one of the sensor via three parameters. In fact, the projection of the target trajectory onto one sensor's observation space can be easily written as:

$$a_i^{(k)} = \frac{\sqrt{P}}{\parallel (\mathbf{x}_0 - \mathbf{x}_s^{(k)}) + t_i \mathbf{v} \parallel} = \frac{a_{\max}^{(k)}}{\sqrt{1 + 3\left(\frac{t_i - t_{\max}^{(k)}}{\Delta t^{(k)}}\right)^2}} \tag{11}$$

with the definitions of the closest approach time and the 6 dB point:

$$t_{\max}^{(k)} = \arg\max_t a^{(k)}(t) \tag{12}$$

$$a_{(k)}\left(t_{\max}^{(k)} \pm \Delta t^{(k)}\right) = \frac{a_{\max}^{(k)}}{2} \tag{13}$$

Inspecting the geometry, c.f. Fig. 3, it can be easily verified that,

$$d_{\min}^{(k)} = \frac{|\tilde{\mathbf{v}}^T(\mathbf{x}_0 - \mathbf{x}_s^{(k)})|}{\parallel \mathbf{v} \parallel}, \quad a_{\max}^{(k)} = \frac{\sqrt{P}}{d_{\min}^{(k)}},$$

$$t_{\max}^{(k)} \cdot \parallel \mathbf{v} \parallel = \frac{\mathbf{v}^T(\mathbf{x}_0 - \mathbf{x}_s^{(k)})}{\parallel \mathbf{v} \parallel}, \quad \Delta t^{(k)} \cdot \parallel \mathbf{v} \parallel = \sqrt{3} d_{\min}^{(k)}, \tag{14}$$

where $\tilde{\mathbf{v}}$ is defined via $\mathbf{v}^T \tilde{\mathbf{v}} = 0$ and $\parallel \tilde{\mathbf{v}} \parallel = \parallel \mathbf{v} \parallel$.

Based on the local measurements, each sensor estimates the parameter vector $\boldsymbol{\psi}^{(k)} = [a_{\max}^{(k)},\, t_{\max}^{(k)},\, \Delta t^{(k)}]$. The ML estimate of the parameter vector $\boldsymbol{\psi}^{(k)}$ is

$$\boldsymbol{\psi}_{\text{ML}}^{(k)} = \arg\max_{\boldsymbol{\psi}^{(k)}} \prod_i f\left(r_i^{(k)} \mid \boldsymbol{\psi}^{(k)}\right). \tag{15}$$

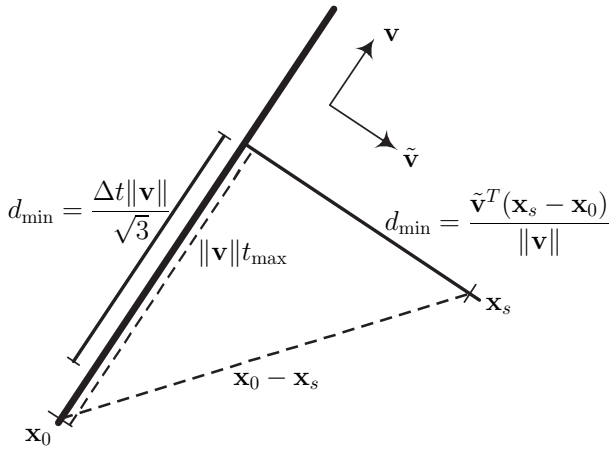

Fig. 3. Given the target's initial position and speed ($\mathbf{x}_0$, $\mathbf{v}$), as well as a sensor location $\mathbf{x}_s$, the closest-point-of-approach (CPA), defined by corresponding time, $t_{\max}$, and distance, $d_{\min}$, can be calculated by considering the geometry.

Then each sensor forwards the three dimensional vector $\boldsymbol{\psi}_{\text{ML}}^{(k)}$ to the FC.

The CRLB of the local estimates can be calculated in a similar fashion as the measurement model stays unchanged. The FIM is

$$J_{\boldsymbol{\psi}}^{(k)} = \frac{1}{\sigma^2} \sum_i \left[\nabla_{\boldsymbol{\psi}} a_i^{(k)}\right] \left[\nabla_{\boldsymbol{\psi}} a_i^{(k)}\right]^T, \tag{16}$$

with the only difference being the derivatives taken with respect to $\boldsymbol{\psi}$,

$$\nabla_{\boldsymbol{\psi}} a_i^{(k)} = \begin{bmatrix} \frac{\partial a_i^{(k)}}{\partial a_{\max}^{(k)}} \\ \frac{\partial a_i^{(k)}}{\partial t_{\max}^{(k)}} \\ \frac{\partial a_i^{(k)}}{\partial \Delta t^{(k)}} \end{bmatrix} = \begin{bmatrix} \frac{1}{\sqrt{1+3\left(\frac{t_{\max}^{(k)} - t_i}{\Delta t^{(k)}}\right)^2}} \\ -\frac{3a_{\max}^{(k)}\left(t_{\max}^{(k)} - t_i\right)\Delta t^{(k)}}{\left[\Delta t^{(k)}\sqrt{1+3\left(\frac{t_{\max}^{(k)} - t_i}{\Delta t^{(k)}}\right)^2}\right]^3} \\ \frac{3a_{\max}^{(k)}\left(t_{\max}^{(k)} - t_i\right)^2}{\left[\Delta t^{(k)}\sqrt{1+3\left(\frac{t_{\max}^{(k)} - t_i}{\Delta t^{(k)}}\right)^2}\right]^3} \end{bmatrix}. \tag{17}$$

B. Fusion Center Processing

We would like to formulate a global cost function, similar to a ML estimator. Then we can choose an estimate $\widehat{\boldsymbol{\theta}}$, which reproduces all information received from the sensors in some closest sense. We define a global cost-function as:

$$\widehat{\boldsymbol{\theta}} = \arg\min_{\boldsymbol{\theta}} \sum_k \left(\boldsymbol{\psi}_{\text{ML}}^{(k)} - \widehat{\boldsymbol{\psi}}^{(k)}(\boldsymbol{\theta})\right)^T J_{\boldsymbol{\psi}}^{(k)} \left(\boldsymbol{\psi}_{\text{ML}}^{(k)} - \widehat{\boldsymbol{\psi}}^{(k)}(\boldsymbol{\theta})\right), \tag{18}$$

where the predicted measurements of sensor k, given a certain target state estimate, $\widehat{\boldsymbol{\psi}}^{(k)}(\boldsymbol{\theta})$, can be found easily from (14):

$$\widehat{\boldsymbol{\psi}}^{(k)}(\boldsymbol{\theta}) = \begin{bmatrix} \hat{a}_{\max}^{(k)} \\ \hat{t}_{\max}^{(k)} \\ \widehat{\Delta t}^{(k)} \end{bmatrix} = \begin{bmatrix} \frac{\sqrt{P}\|\mathbf{v}\|}{|\tilde{\mathbf{v}}^T(\mathbf{x}_0 - \mathbf{x}_s^{(k)})|} \\ \frac{\mathbf{v}^T(\mathbf{x}_0 - \mathbf{x}_s^{(k)})}{\|\mathbf{v}\|^2} \\ \sqrt{3}\frac{|\tilde{\mathbf{v}}^T(\mathbf{x}_0 - \mathbf{x}_s^{(k)})|}{\|\mathbf{v}\|^2} \end{bmatrix} \tag{19}$$

Note that the cost function (18) is equivalent to assuming that the local sensor estimates $\boldsymbol{\psi}_{\text{ML}}^{(k)}$ are corrupted by additive Gaussian noise, their covariance given by the FIM. This is of course not correct, but seems to work reasonably in practice. The FIM, $J_{\boldsymbol{\psi}}^{(k)}$, is evaluated at the local estimates $\boldsymbol{\psi}_{\text{ML}}^{(k)}$, so no additional data has to be transmitted.

The minimization in (18) is a heavily non-linear least squares problem. To avoid exhaustive search, we need a good initial estimate – then we will have a good chance to reach a global maximum via simple gradient based optimization. In the following we will find a closed form estimate based on two sensors, by assuming noiseless measurements $\boldsymbol{\psi}^{(k)}$ and solving the geometrical problem.

1) Initial Estimate Based on Two Sensors: As noted before, based on two sensors, there are four possible target trajectories. Two interior solutions, c.f. Fig. 2(a), and two exterior solutions, c.f. Fig 2(b).

a) Interior solutions: The interior intersection point $\tilde{\mathbf{p}}_{\text{in}}$ can be calculated using the following ratio,

$$\eta := d_{\text{min}}^{(1)} / d_{\text{min}}^{(2)} = a_{\text{max}}^{(2)} / a_{\text{max}}^{(1)} \tag{20}$$

as the weighted average of the sensor locations,

$$\tilde{\mathbf{p}}_{\text{in}} = \frac{d_{\text{min}}^{(2)}\mathbf{x}_s^{(1)} + d_{\text{min}}^{(1)}\mathbf{x}_s^{(2)}}{d_{\text{min}}^{(1)} + d_{\text{min}}^{(2)}} = \frac{\mathbf{x}_s^{(1)} + \eta\mathbf{x}_s^{(2)}}{1+\eta}. \tag{21}$$

Similarly the time when the target would pass through this point can be calculated from the times of closest approach $t_{\text{max}}^{(k)}$,

$$\tilde{t}_{\text{in}} = \frac{t_{\text{max}}^{(1)} + \eta t_{\text{max}}^{(2)}}{1+\eta}. \tag{22}$$

Using this as a reference point, we can find two possible velocity vectors, c.f. Fig. 2(a); using the definitions in (14),

$$\left(t_{\text{max}}^{(1)} - t_{\text{max}}^{(2)}\right) \cdot \| \mathbf{v} \| = \frac{\mathbf{v}^T(\mathbf{x}_0 - \mathbf{x}_s^{(1)})}{\| \mathbf{v} \|} - \frac{\mathbf{v}^T(\mathbf{x}_0 - \mathbf{x}_s^{(2)})}{\| \mathbf{v} \|} \tag{23}$$

$$= \frac{\mathbf{v}^T(\mathbf{x}_s^{(2)} - \mathbf{x}_s^{(1)})}{\| \mathbf{v} \|} \tag{24}$$

$$= \| \mathbf{x}_s^{(2)} - \mathbf{x}_s^{(1)} \| \cos\beta \tag{25}$$

where β is the angle between the velocity vector, $\mathbf{v}$, and the line connecting the locations of the sensors, $(\mathbf{x}_s^{(2)} - \mathbf{x}_s^{(1)})$. Further we can use

$$\left(\Delta t^{(1)} + \Delta t^{(2)}\right) \cdot \| \mathbf{v} \| = \sqrt{3}\frac{\tilde{\mathbf{v}}^T(\mathbf{x}_s^{(2)} - \mathbf{x}_s^{(1)})}{\| \mathbf{v} \|} = \sqrt{3} \| \mathbf{x}_s^{(2)} - \mathbf{x}_s^{(1)} \| \sin\beta \tag{26}$$

and we choose $\tilde{\mathbf{v}}$ such that $\tilde{\mathbf{v}}^T(\mathbf{x}_0 - \mathbf{x}_s^{(2)}) < 0 < \tilde{\mathbf{v}}^T(\mathbf{x}_0 - \mathbf{x}_s^{(1)})$, which we can since the target is assumed to pass between the sensors (the definitions match Fig. 2(a) / Fig. 3). It follows

$$\tan\beta = \sqrt{3}\frac{\Delta t^{(1)} + \Delta t^{(2)}}{t_{\text{max}}^{(1)} - t_{\text{max}}^{(2)}}, \tag{27}$$

$$\| \mathbf{v} \| = \frac{\| \mathbf{x}_s^{(2)} - \mathbf{x}_s^{(1)} \|}{t_{\text{max}}^{(1)} - t_{\text{max}}^{(2)}} \cos\beta, \tag{28}$$

where the tangent has an ambiguity leading to two possible solutions. The original reference point can be reconstructed based on the velocity vector and the interior point

$$\mathbf{x}_0 = \tilde{\mathbf{p}}_{\text{in}} - \tilde{t}_{\text{in}}\mathbf{v}. \tag{29}$$

b) Exterior solutions: The exterior intersection point can be calculated similarly as,

$$\tilde{\mathbf{p}}_{\text{ex}} = \frac{\mathbf{x}_s^{(1)} - \eta\mathbf{x}_s^{(2)}}{1-\eta}, \tag{30}$$

with the corresponding time,

$$\tilde{t}_{\text{ex}} = \frac{t_{\max}^{(1)} - \eta t_{\max}^{(2)}}{1-\eta}. \tag{31}$$

Otherwise the equations stay similar, with a new angle γ,

$$\left(t_{\max}^{(1)} - t_{\max}^{(2)}\right) \cdot \| \mathbf{v} \| = \| \mathbf{x}_s^{(2)} - \mathbf{x}_s^{(1)} \| \cos\gamma, \tag{32}$$

but now both sensors lie on the same side of the trajectory (same sign),

$$\left(\Delta t^{(1)} - \Delta t^{(2)}\right) \cdot \| \mathbf{v} \| = \sqrt{3} \| \mathbf{x}_s^{(2)} - \mathbf{x}_s^{(1)} \| \sin\gamma. \tag{33}$$

The solutions are:

$$\tan\gamma = \sqrt{3}\frac{\Delta t^{(1)} - \Delta t^{(2)}}{t_{\max}^{(1)} - t_{\max}^{(2)}}, \tag{34}$$

$$\| \mathbf{v} \| = \frac{\| \mathbf{x}_s^{(2)} - \mathbf{x}_s^{(1)} \|}{t_{\max}^{(1)} - t_{\max}^{(2)}} \cos\gamma, \tag{35}$$

and

$$\mathbf{x}_0 = \tilde{\mathbf{p}}_{\text{ex}} - \tilde{t}_{\text{ex}}\mathbf{v}. \tag{36}$$

2) Multiple Starting Points: Having reduced data sets $\boldsymbol{\psi}_{\text{ML}}^{(k)}$ from two sensors, there are still four ambiguous solutions. One variant is to start gradient based optimization from each solution and compare the cost function at the end points. Reduced complexity can be achieved by choosing the lowest cost function among the four starting points, reducing the complexity spent on the gradient based optimization by a factor of four, but possibly degrading performance.

Consider three sensors; there are three possible sensor pairs. Each pair gives four solutions, leading to a total of twelve initial points. As this number grows exponentially with the number of sensors, either a clustering algorithm can be applied to reduce cost function evaluations by grouping solutions together that will converge most likely to the same end point (as in [14]), or a preferable pair of sensors could be chosen for initialization, e.g., based on their FIMs.

IV. Numerical Results

A. Scenario Description

Based on the previous discussion, each sensor locally estimates a three-parameter vector $\boldsymbol{\psi}_{\text{ML}}^{(k)}$ and forwards it to the FC. The FC then estimates the target trajectory based on the data delivered by the sensors as described in Section III-B.

The scenario we consider for illustration is shown in Fig. 4; the target passes through a sensor field, where we will consider a varying number of sensors (indicated by different markers in the figure). As the minimum number of sensors to arrive at an unambiguous estimate is three, we will start with only three sensors, gradually increasing this until all twenty sensors shown in Fig. 4 are included. This will also indicate a further tradeoff between communication load and estimation accuracy, as even in a large sensor field only a subset of sensors could be queried for sensor readings to preserve battery power or available bandwidth.

The range between the sensors and the target is on the order of kilometers, the measurement sampling frequency is 1 Hz and the target's speed is approximately $\| \mathbf{v} \| \approx 200$ m/s, which would be an aircraft in a radar scenario, but could easily be adapted to slower speeds and longer observation intervals. The signal-to-noise ratio (SNR) at a reference distance of 1 km is defined as P/σ^2 and is varied between 10-40 dB.

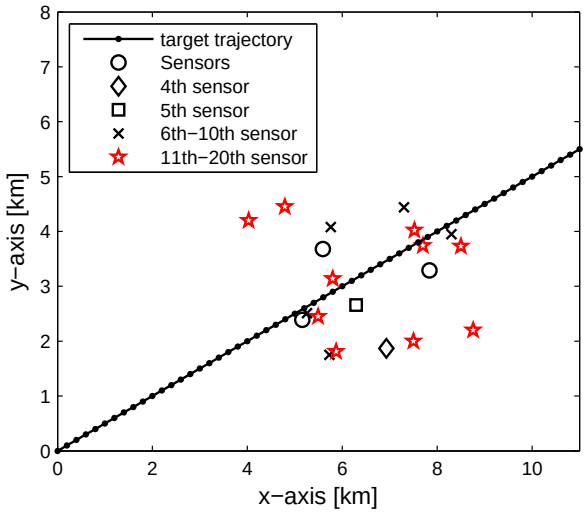

Fig. 4. Overview of the example scenario; the target passes through a sensor field of roughly 4×4 km, subsets of the available sensors will be used at first, to compare estimation accuracy in terms of available sensors (numbering of sensors 1-3, denoted here as "Sensors", is identical to Fig. 1).

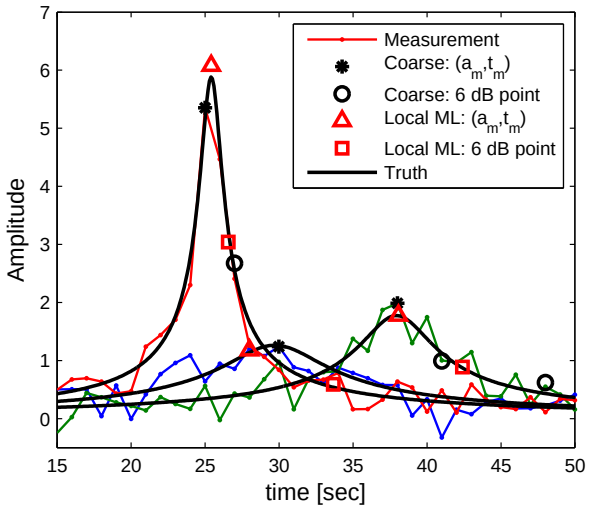

Fig. 5. Example of local sensor estimates for an SNR of 10 dB; shown are the underlying truth, the sensor measurements, the coarse estimates, and the ML estimates $\boldsymbol{\psi}_{\text{ML}}^{(k)}$.

B. Local Sensor Processing

Each sensor processes its observations locally, generating an ML estimate. Since the function in (15) can be multi-modal, in a first step coarse estimates are formed by simply taking the maximum over the received samples and the point closest to half this amplitude (c.f. Fig. 5); from this starting point we use a gradient based non-linear least-squares algorithm to converge to a (local) maximum. As can be seen in Fig. 5, even the coarse estimates are fairly close, so the gradient based ML search usually converges to a global maximum in the AWGN case.

Comparing the CRLB as defined in (16) with Monte-Carlo simulation using 10^3 runs, we can see that the local estimates basically reach the bound on estimation accuracy, c.f. Fig 6. For low SNR a more sophisticated local processing, possibly using a starting point based on interpolation or low pass filtered measurements, could improve performance. The estimation accuracy between the three sensors varies, as some sensors are closer to the target and therefore have a higher received SNR. This is also reflected in the corresponding CRLBs.

C. FC Processing

The FC combines the data generated by sensors and estimates the trajectory, using the cost function in (18). We find that in comparison to a centralized ML-estimator having available all raw sensor measurements, the loss in estimation accuracy is small.

We start with a setup of three sensors, marked in Fig. 4 as circles; although as discussed previously, an unambiguous solution exists, e.g., based on the full ML cost-function in (5), its estimation accuracy described by the CRLB in (3) – to find this solution a five-dimensional non-linear estimation problem has to be solved. The same applies to our cost function in (18). With increasing SNR and number of sensors we expect for both cost functions to become more "benign", i.e., efficient - but sub-optimal - optimization schemes like gradient based approaches, will arrive more often at the global optimum.

In any case, efficient solving of these non-linear optimization problems will strongly depend on the initialization. We take the following approach: each possible sensor pair generates four ambiguous solutions based on the closed form formulas; then all these tentative estimates are evaluated using the cost function in (18), where we expect that solutions connected to "mirror" images are discarded; finally the gradient based optimization is initialized with the tentative estimate with the best cost function value. We expect that if we initialize the gradient based optimization with an estimate connected to a "mirror" image, the final estimate will be poor. Therefore we include a separate statistic: how often a "mirror" image was selected and how good the performance is excluding these cases.

The three sensor case is shown in Fig. 7, we notice that for low to average SNR the performance is degraded by choosing a wrong initialization. As comparison we also include an estimate based on the full ML cost-function in (5), initialized with the same point - therefore also suffering from bad

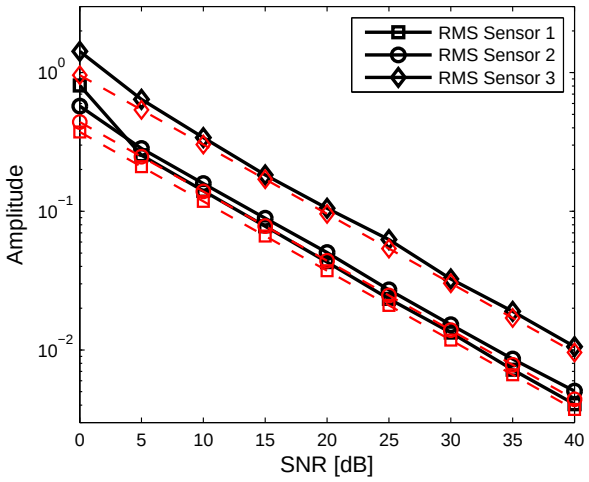

(a) RMSE: amplitude $a_{\max}^{(k)}$

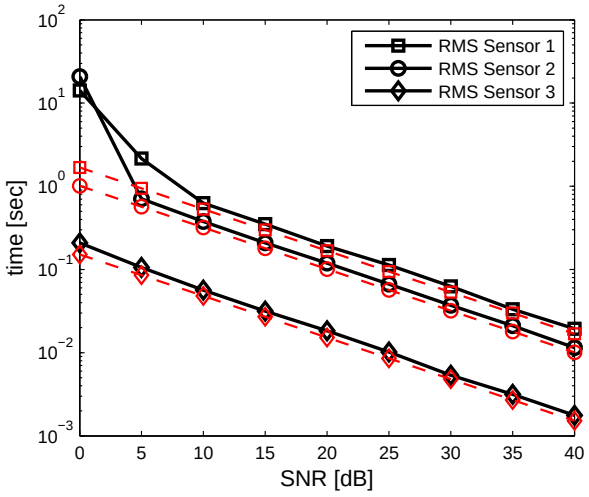

(b) RMSE: time $t_{\max}^{(k)}$

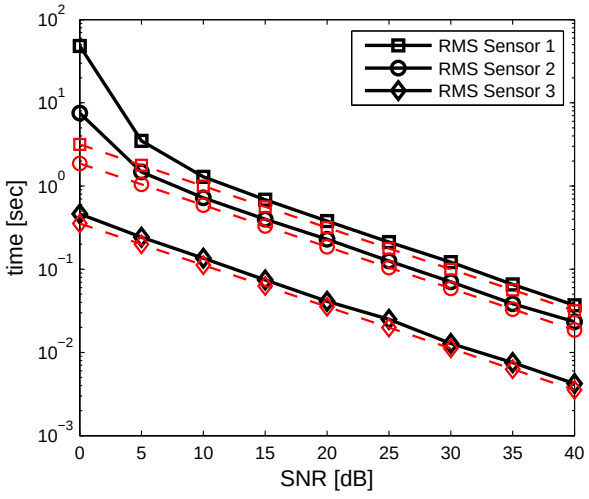

(c) RMSE: time difference $\Delta t^{(k)}$

Fig. 6. Root-mean-square error (RMSE) of local sensor estimate; as comparison the CRLB for each sensor as defined in (16) is included as dashed lines – which is basically met by the local estimates; numbering of sensors 1-3 correponds to Fig. 1.

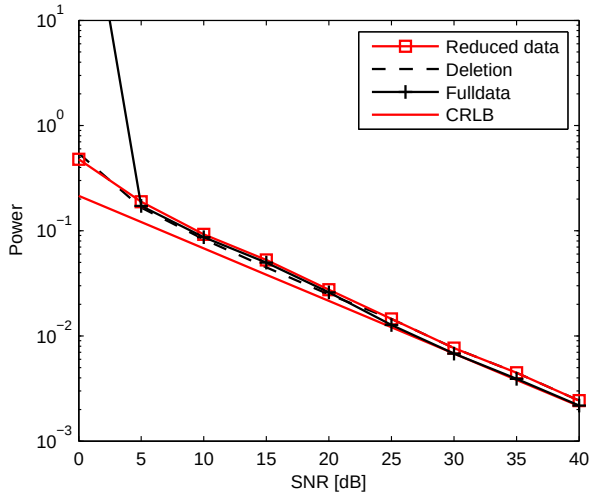

(a) RMSE: Power P

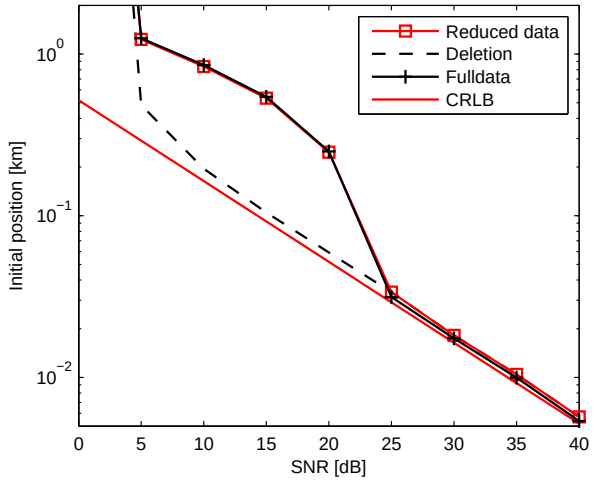

(b) RMSE: Initial position $\mathbf{x}_0$

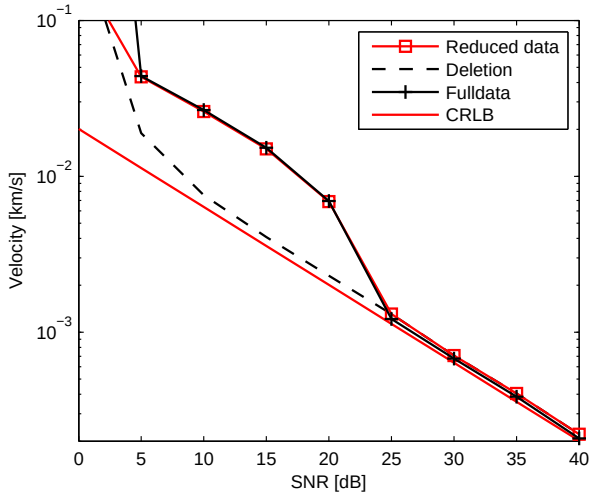

(c) RMSE: Velocity of target $\mathbf{v}$

Fig. 7. Plot of the RMSE for three sensors; the plots include a case where wrong initializations are deleted, solutions based on the total raw sensor measurements and the CRLB as defined in (3); the SNR is defined at a reference distance of 1 km.

intialization. Once the initialization errors become negligible, we see that the full ML solution basically achieves the CRLB, closely followed by the reduced communication scheme.

When using more sensors, initialization complexity increases, as there are more possible sensor pairs. Still, since the initial estimates are based on closed form solutions, the complexity is limited. We consider increasing the number of sensors from three to twenty in several steps, see Fig. 8. As expected more independent observations lead to improved estimation accuracy, as reflected in the CRLB, but for the cases of four or five sensors, the main improvement is related to better initialization. The CRLB only improves slightly, while the errors due to wrong initialization are greatly reduced (position and velocity); we include an additional plot, Fig. 8(a), which shows the probability to initialize from a "mirror" image, instead of including the performance with these cases removed as before. We find that even a slight increase in the number of sensors helps strongly to reduce this probability, because "mirror" images are not common between sensors.

When using a large number of sensors, estimation accuracy improves slowly. As the received SNR is inversely proportional to the distance to the target, the sensors which are close to the target trajectory dominate the performance. In this sense a dense sensor network simply increases the chance of having a sufficient number of sensors close to the target trajectory, while not necessarily all sensors need to transmit to the FC. For example, only sensors with a sufficiently large $a_{\text{max}}^{(k)}$ could transmit their data; but we do not pursue this idea further here.

V. Extension to Rayleigh Model

Assuming a Rayleigh fading signal model (Swerling II target), the amplitude measurements are given by

$$r_i^{(k)} = h_i^{(k)} \cdot a_i^{(k)} + w_i^{(k)}, \tag{37}$$

where the $h_i^{(k)}$ and $w_i^{(k)}$ are zero-mean complex Gaussian random variables of unit and N_0 variance respectively. The measurements $r_i^{(k)}$ are therefore complex Gaussian, their amplitude is Rayleigh distributed

$$f\left(|r_i^{(k)}||\boldsymbol{\psi}^{(k)}\right) = \frac{2|r_i^{(k)}|}{N_0 + (a_i^{(k)})^2} \exp\left(-\frac{|r_i^{(k)}|^2}{N_0 + (a_i^{(k)})^2}\right); \tag{38}$$

while the phase is uniform and holds no information.

The optimal centralized solution is the ML estimate given by,

$$\boldsymbol{\theta}_{\text{ML}} = \arg\max_{\boldsymbol{\theta}} \prod_{k,i} f\left(|r_i^{(k)}| \,|\, \boldsymbol{\theta}\right), \tag{39}$$

but the probability density function is now given by (38). The CRLB on the estimation accuracy can be calculated via the FIM,

$$J_{\boldsymbol{\theta}} = \sum_{k,i} \left(\frac{2a_i^{(k)}}{N_0 + (a_i^{(k)})^2}\right)^2 \left[\nabla_{\boldsymbol{\theta}} a_i^{(k)}\right] \left[\nabla_{\boldsymbol{\theta}} a_i^{(k)}\right]^T, \tag{40}$$

where the gradients are unchanged from (5). Interestingly, and opposed to the AWGN result, the FIM for a given geometry is bounded. While in (16) the FIM has a leading term inversely

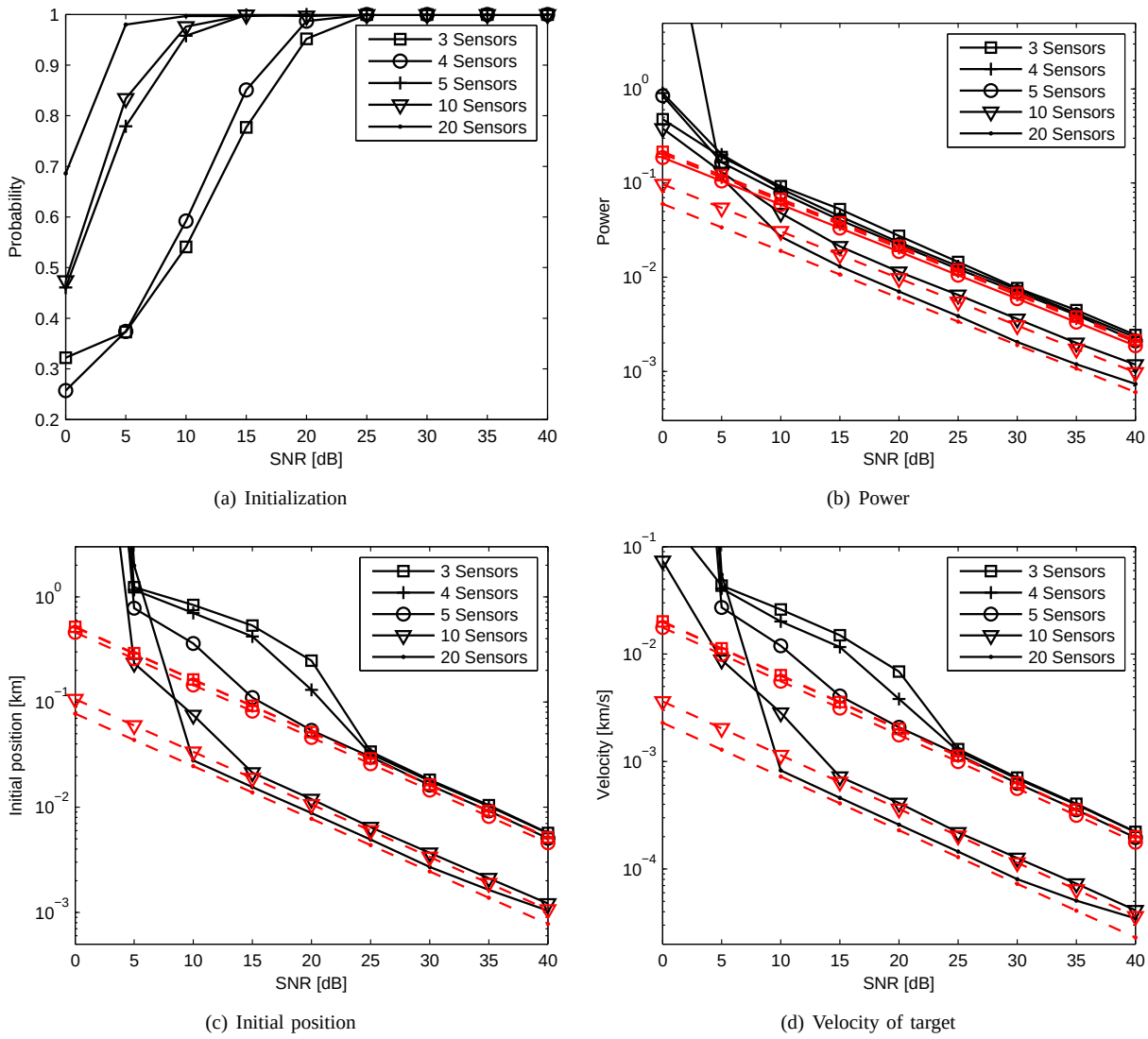

(a) Initialization

(b) Power

(c) Initial position

(d) Velocity of target

Fig. 8. Comparison for varying number of sensors; (a) probability of not choosing a "mirror" image for initialization; (b)-(d) about five sensors are sufficient for performance close to the CRLB (dashed lines), while larger numbers bring only gradual improvement.

proportional to the noise variance, here the leading terms approach constant values when the noise variance diminishes, therefore for a given geometry the performance will not improve beyond a certain point, even for infinite SNR.

A. Adapted Sensor Processing

The local sensor processing is the same in principle, but each sensor calculates the ML estimates of the parameter vector $\boldsymbol{\psi}^{(k)} = [a_{\max}^{(k)},\, t_{\max}^{(k)},\, \Delta t^{(k)}]$ using the Rayleigh probability density,

$$\boldsymbol{\psi}_{\mathrm{ML}}^{(k)} = \arg\max_{\boldsymbol{\psi}^{(k)}} \prod_i f\left(|r_i^{(k)}| \,|\, \boldsymbol{\psi}^{(k)}\right). \tag{41}$$

The calculation of the CRLB also uses the Rayleigh probability density; the FIM can be calculated as

$$J_{\boldsymbol{\psi}^{(k)}} = \sum_i \left(\frac{2a_i^{(k)}}{N_0 + (a_i^{(k)})^2}\right)^2 \left[\nabla_{\boldsymbol{\psi}} a_i^{(k)}\right] \left[\nabla_{\boldsymbol{\psi}} a_i^{(k)}\right]^T, \tag{42}$$

where the definition of the gradient $\nabla_{\boldsymbol{\psi}} a_i^{(k)}$ is in (17). The same observation concerning the noise variance applies as for the centralized CRLB.

The estimates are forwarded to the FC as before; the processing at the FC is not affected by the measurement model, except for the evaluation of the local FIMs, necessary for the cost function in (18). We will study some numerical examples in the following.

B. Numerical Results

The Rayleigh fading model is in some sense the most challenging, as our only information about the target is contained in the amplitude - now severely distorted by fading. This is reflected in the CRLB, as even for $N_0 \to 0$, the CRLB does not improve beyond a certain point, dictated by the number of measurements and sensors. To achieve any reasonable performance, we need to increase the measurement rate, which we first double to 2 Hz.

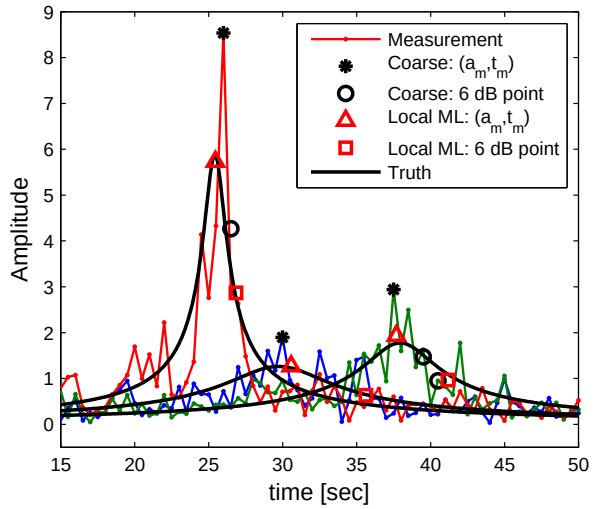

Fig. 9. Example of the Rayleigh fading model; the amplitude information is severely distorted making this measurement model very challenging.

To visualize this challenging scenario, we plot the same example from Fig. 5 now for the Rayleigh fading model in Fig. 9. We immediately notice that the amplitude is barely observable, noticeable especially at the coarse estimates. The local processing has to be either performed via a grid search in three-dimensional space, or improved initial estimates have to be acquired using some smoothing operation. To start the gradient based optimization, we use coarse estimates obtained after filtering the received data with a Gaussian shape low-pass filter.

The results for the local processing are shown in Fig. 10(a)-(c), where in comparison with Fig. 6 we see a very contrasting behavior in the CRLB. As mentioned before the FIM is bounded from above for increasing SNR; this is now reflected in the CRLBs being bounded from below. Generally the performance is lower than in the equivalent AWGN scenario, even though we have double the number of measurements. Still, the local processing achieves the CRLB and can therefore be characterized by the respective FIMs.

In Fig. 11(a) we plot the estimation accuracy for varying numbers of sensors; we limit the plot to the initial position $\mathbf{x}_0$ as the plot for the velocity $\mathbf{v}$ has largely similar behavior and the source level P is only a nuisance parameter. We see that the performance does not reach the CRLB, especially so for small numbers of sensors. As the local estimates are of low accuracy, the global cost function has many local maxima of similar height to the true solution. Only for five or more sensors can a good initialization point be chosen reliably, see Fig. 11(b).

Next we consider the same setup, but increase the local sensor measurement rate to 10 Hz. In Fig. 12 we see that this greatly improves performance; looking at the CRLB we improve as predicted by a little more than 6 dB, due to having five times as many measurements, more or less linearly scaling the FIM. Much more important, the initialization and global optimization improves so that five or more sensors lead to a negligible number of bad initializations.

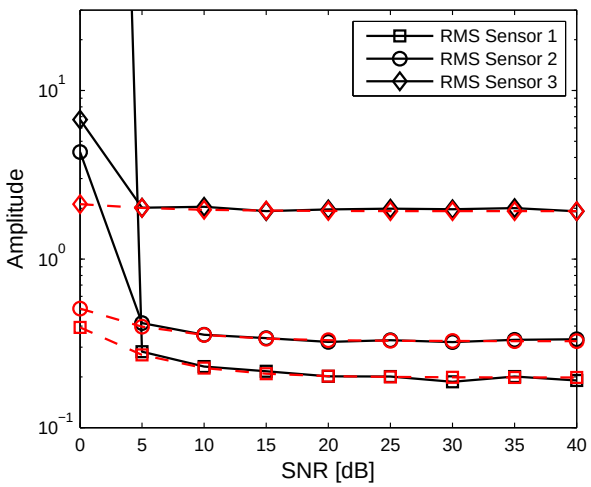

(a) Amplitude $a_{\max}^{(k)}$

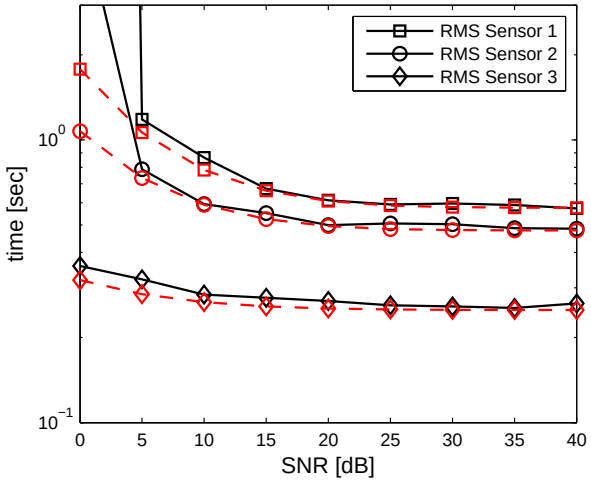

(b) Time $t_{\max}^{(k)}$

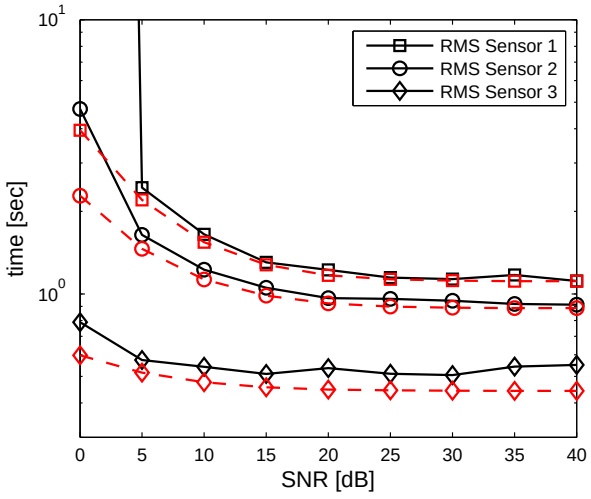

(c) Time Difference $\Delta t^{(k)}$

Fig. 10. Plot of local RMSE and CRLB for the Rayleigh measurement model; the performance is generally worse than for AWGN and does not increase significantly with SNR. Still the local ML estimates are close to the bounds.

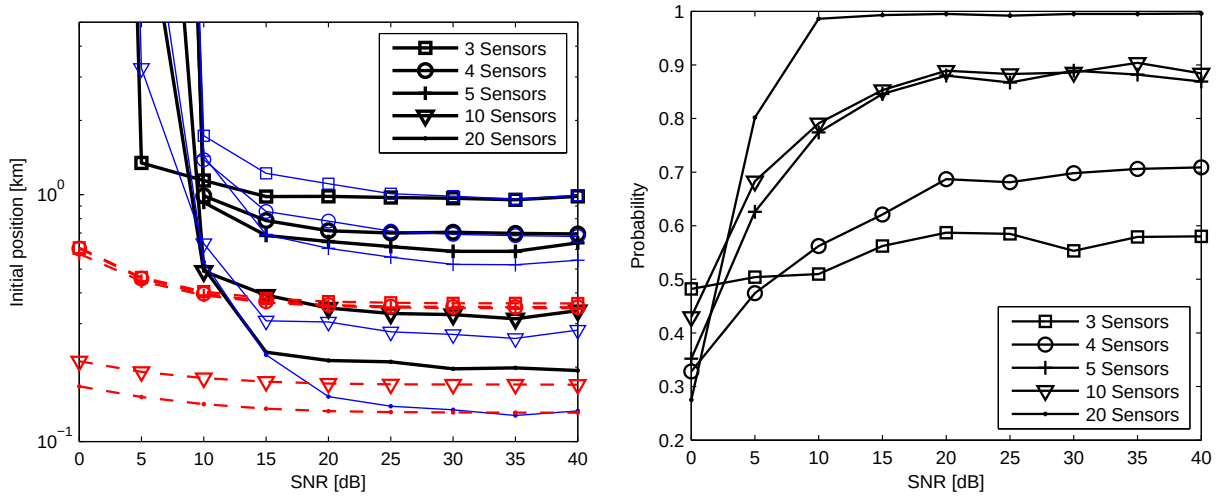

(a) Initial Position $\mathbf{x}_0$ (b) Initialization

Fig. 11. As an example we plot (a) the RMSE of the initial position (thick lines are based on reduced data, thin lines are basd on full raw data, dashed lines are CRLB) and (b) the probaility of correct initialization for the Rayleigh measurement model with rate of 2 Hz.

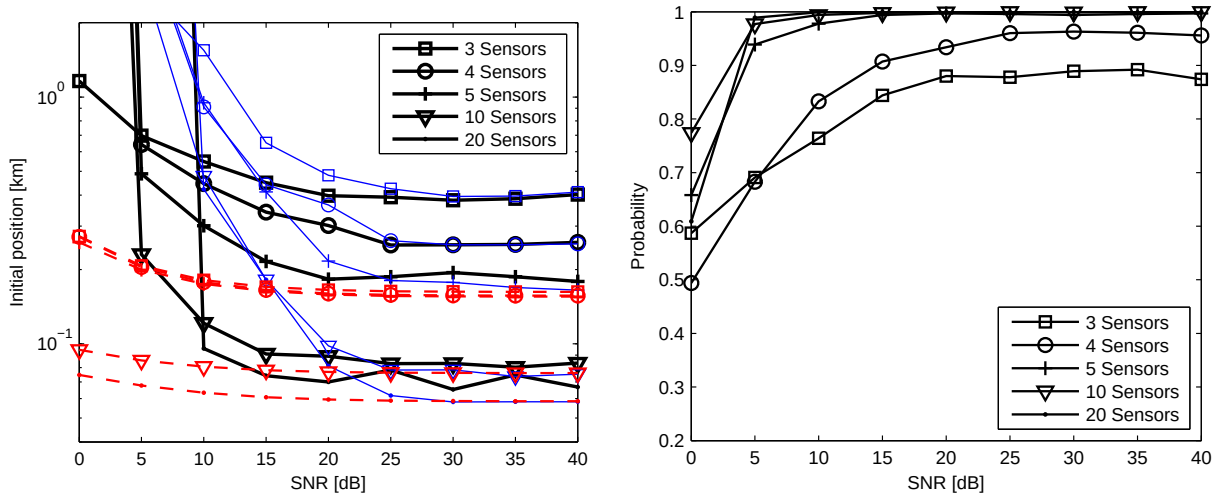

(a) Initial Position $\mathbf{x}_0$ (b) Initialization

Fig. 12. Increasing the measurement rate to 10 Hz, the performance can be improved to values comparable to the AWGN case at 1 Hz and average SNR (thick lines are based on reduced data, thin lines are basd on full raw data, dashed lines are CRLB).

VI. Conclusion

We studied a scenario in which a target moves through a sensor field at constant velocity. The sensors are simple in that they can only measure a received signal strength (RSS) profile, which is modeled using a free-space attenuation model. Subject to a low communication rate, the target trajectory is to be estimated at a fusion center (FC). We suggest the following approach to this end: the sensors locally process their measurements, extracting three characteristic parameters using local maximum likelihood (ML) estimtes, namely i) the maximum measured amplitude, corresponding to the closest-point-of-approach (CPA); ii) the corresponding time index; and iii) the time it takes for the expected amplitude to diminish by 6 dB relative to that at the CPA. Each sensor only transmits these three characteristic values to the FC, independent of the number of local raw measurements. The FC combines these reduced data sets, using a ML-like approach, which we initialize using geometric considerations. We find that this approach leads to a much reduced communication load, achieves estimation performance close to the centralized estimator using all raw measurements and can be easily adapted to varying measurement models, e.g., additive white Gaussian noise (AWGN) or Rayleigh fading. Surprisingly, this approach also benefits from an increased measurement frequency at the local sensors, where more raw data is available; although no additional data is transmitted, the improved local estimates lead to a greatly improved final performance.

References

[1] S. Haykin, *Array Signal Processing*. Englewood-Cliffs, NJ: Prentice-Hall, 1985.

[2] H. Van Trees, *Optimum Array Processing*, 1st ed., ser. Detection, Estimation, and Modulation Theory (Part IV). New York: John Wiley & Sons, Inc., 2002.
[3] D. Li, K. D. Wong, Y. H. Hu, and A. M. Sayeed, "Detection, classification, and tracking of targets," *IEEE Signal Processing Magazine*, vol. 19, no. 2, pp. 17–29, May 2002.
[4] D. C. Reid, A. M. Zoubir, and B. Boashash, "The bootstrap applied to passive acoustic aircraft parameter estimation," in *Proc. of Intl. Conf. on Acoustics, Speech and Signal Proc.*, vol. 6, Atlanta, GA, May 1996, pp. 3153–3156.
[5] R. F. Brcich and A. M. Zoubir, "The use of the DPT in passive acoustic aircraft flight parameter estimation," in *Proc. IEEE Region 10 Annual Conference; Speech and Image Technologies for Computing and Telecommunications*, vol. 2, Dec. 1997, pp. 819–822.
[6] R. J. Kozick and B. M. Sadler, "Source localization with distributed sensor arrays and partial spatial coherence," in *Proc. SPIE 2000 AeroSense Symp.*, Orlando, FL, Apr. 2002, pp. 142–153.
[7] ——, "Tracking moving acoustic sources with a network of sensors," Army Research Laboratory, Technical Report ARL-TR-2750, Oct. 2002.
[8] Y. H. Hu and D. Li, "Energy based collaborative source localization using acoustic micro-sensor array," in *Proc. of IEEE Workshop on Multimedia Signal Proc.*, Dec. 2002, pp. 371–375.
[9] X. Sheng and Y.-H. Hu, "Maximum likelihood multiple-source localization using acoustic energy measurements with wireless sensor networks," *IEEE Trans. Signal Processing*, vol. 53, no. 1, pp. 44–53, Jan. 2005.
[10] D. Blatt and A. Hero, "Energy-based sensor network source localization via projection onto convex sets," *IEEE Trans. Signal Processing*, vol. 54, no. 9, pp. 3614–3619, Sep. 2006.
[11] R. Niu and P. K. Varshney, "Target location estimation in sensor networks with quantized data," *IEEE Trans. Signal Processing*, vol. 12, no. 54, pp. 4519–4528, Dec. 2006.
[12] Y. H. Kim and A. Ortega, "Maximum a posteriori (MAP)-based algorithm for distributed source localization using quantized acoustic sensor readings," in *Proc. of Intl. Conf. on Acoustics, Speech and Signal Proc.*, May 2006, pp. V/1053–V/1056.
[13] S. Zhou and P. Willett, "Submarine location estimation via a network of detection-only sensors," *IEEE Trans. Signal Processing*, vol. 55, no. 6, pp. 3104–3115, Jun. 2007.
[14] T. Wettergren, R. Streit, and J. Short, "Tracking with distributed sets of proximity sensors using geometric invariants," *IEEE Trans. Aerosp. Electron. Syst.*, vol. 40, no. 4, pp. 1366–1374, Oct. 2004.
[15] X. Wang and D. Musicki, "Target tracking using energy based detections," in *Proc. of Intl. Conf. on Information Fusion*, Jul. 2007.
[16] S. Choi, C. R. Berger, S. Zhou, and P. Willett, "Estimation of target trajectories based on distributed channel energy measurements," in *Proc. of Intl. Conf. on Information Fusion*, Cologne, Germany, Jul. 2008.
[17] H. Van Trees, *Detection, Estimation, and Modulation Theory*, 1st ed. New York: John Wiley & Sons, Inc., 1968.
[18] H. Dörrie, *100 Great Problems of Elementary Mathematics: Their History and Solution.* New York: Dover Publications, 1965.

PLACE PHOTO HERE

Christian R. Berger (S'05–M'09) was born in Heidelberg, Germany, on September 12, 1979. He received the Dipl.-Ing. degree from the Universität Karlsruhe (TH), Karlsruhe, Germany in 2005, and the Ph.D. degree from the University of Connecticut, Storrs, both in electrical engineering.

In the summer of 2006, he was as a visiting scientist at the Sensor Networks and Data Fusion Department of the FGAN Research Institute, Wachtberg, Germany. He is currently a post-doctoral researcher at the Department of Electrical and Computer Engineering, Carnegie Mellon University, Pittsburgh, USA. His research interests lie in the areas of communications and signal processing, including distributed estimation in wireless sensor networks, wireless positioning and synchronization, underwater acoustic communications and networking.

Dr. Berger has served as a reviewer for the IEEE Transactions on Signal Processing, Wireless Communications, Vehicular Technology, and Aerospacespace and Electronic Systems. In 2008 he was member of the technical program committee and session chair for the 11th International Conference on Information Fusion in Cologne, Germany.

PLACE PHOTO HERE

Sora Choi (S'08) received the M.S and Ph.D. degrees, both in Mathematics, from Seoul National University, Seoul, Korea in 1998 and 2003 respectively. From 2003 to 2004 she was a researcher in the Electronics and Telecommunications Research Institute (ETRI), Daejeon, Korea. She is currently a graduate student/research assistant with University of Connecticut, Storrs, where she is pursuing the Ph.D. degree in Electrical Engineering. Her research interests are generally in target tracking, detection theory, and signal processing.

PLACE PHOTO HERE

Shengli Zhou (M'03) received the B.S. degree in 1995 and the M.Sc. degree in 1998, from the University of Science and Technology of China (USTC), Hefei, both in electrical engineering and information science. He received his Ph.D. degree in electrical engineering from the University of Minnesota (UMN), Minneapolis, in 2002.

He has been an assistant professor with the Department of Electrical and Computer Engineering at the University of Connecticut (UCONN), Storrs, 2003-2009, and now is an associate professor. He holds a United Technologies Corporation (UTC) Professorship in Engineering Innovation, 2008-2011. His general research interests lie in the areas of wireless communications and signal processing. His recent focus is on underwater acoustic communications and networking.

Dr. Zhou has served as an associate editor for IEEE Transactions on Wireless Communications from Feb. 2005 to Jan. 2007, and is now an associate editor for IEEE Transactions on Signal Processing. He received the 2007 ONR Young Investigator award and the 2007 Presidential Early Career Award for Scientists and Engineers (PECASE).

PLACE PHOTO HERE

Peter Willett (F'03) received his BASc (Engineering Science) from the University of Toronto in 1982, and his PhD degree from Princeton University in 1986.

He has been a faculty member at the University of Connecticut ever since, and since 1998 has been a Professor. His primary areas of research have been statistical signal processing, detection, machine learning, data fusion and tracking. He has interests in and has published in the areas of change/abnormality detection, optical pattern recognition, communications and industrial/security condition monitoring.

Dr. Willett is editor-in-chief for IEEE Transactions on Aerospace and Electronic Systems, and until recently was associate editor for three active journals: IEEE Transactions on Aerospace and Electronic Systems (for Data Fusion and Target Tracking) and IEEE Transactions on Systems, Man, and Cybernetics, parts A and B. He is also associate editor for the IEEE AES Magazine, editor of the AES Magazines periodic Tutorial issues, associate editor for ISIFs electronic Journal of Advances in Information Fusion, and is a member of the editorial board of IEEEs Signal Processing Magazine. He has been a member of the IEEE AESS Board of Governors since 2003. He was General Co- Chair (with Stefano Coraluppi) for the 2006 ISIF/IEEE Fusion Conference in Florence, Italy, Program Co-Chair (with Eugene Santos) for the 2003 IEEE Conference on Systems, Man, and Cybernetics in Washington DC, and Program Co-Chair (with Pramod Varshney) for the 1999 Fusion Conference in Sunnyvale.